

Scanning eddy current dynamometer with 100 μm resolution

B. S. Palmer, H. D. Drew, and R. S. Decca^{a)}

Laboratory for Physical Sciences and Department of Physics, University of Maryland, College Park, Maryland 20740

(Received 3 November 1999; accepted for publication 25 April 2000)

We report on a new contactless scanning probe technique to probe thin metallic films. The scanning eddy current dynamometer (SECD) is based on the measurement of the force generated by a magnetic tip oscillating in close proximity to a conducting thin film glued to a high- Q mechanical oscillator. By measuring the resonant motion induced in the mechanical oscillator, the eddy current force on the sample can be determined. The size of the magnetic field profile from our tip limits the spatial resolution of the instrument to $\approx 100 \mu\text{m}$. This spatial resolution is demonstrated by scanning the magnetic tip over inhomogeneities in metallic films. For a homogeneous metallic film much larger than $100 \mu\text{m}$ the force measured by the SECD is directly proportional to the conductance of the film. In this configuration the equivalent noise conductance of the eddy current dynamometer is $\Delta\sigma_{\square} \approx 30 \Omega^{-1}$. By exploiting the boundary conditions on the induced current density in the conducting film, cracks much smaller than $100 \mu\text{m}$ in a metallic film can be detected. To demonstrate this property, a $2.5 \mu\text{m}$ wide slit is detected using the SECD. © 2000 American Institute of Physics. [S0034-6748(00)00608-0]

I. INTRODUCTION

Eddy current testing is widely used as a nondestructive technique for mapping and detecting defects in conducting materials. Eddy current probes commonly use a coil to induce the eddy currents in the conducting layer and the currents are detected either by using a second coil,¹ by monitoring the impedance in the first coil,¹ or by using a superconducting quantum interference device (SQUID) to measure the magnetic flux from the eddy currents.² In this article we use a different approach, based in recent developments on the detection of small forces.

Ultrasmall force detection using mechanical oscillators has made it possible to construct very sensitive electrometers³ and magnetometers.⁴ These instruments utilize mechanical oscillators made from Si having quality factors on the order of 10^6 . In this article we describe a new microprobe instrument to measure eddy current forces on thin metallic films based on Si mechanical oscillators. The eddy currents are induced by moving a magnetic probe over the sample which is mounted on a Si oscillator. We refer to this device as a scanning eddy current dynamometer (SECD). The advantage of our instrument is that it has a spatial resolution on the order of $100 \mu\text{m}$ and could be potentially improved to have a spatial resolution on the order of $1 \mu\text{m}$.

To gain insight into the nature of the eddy current force on a thin film due to a moving magnetic probe, consider a direct current (dc) loop held parallel over a thin infinite sheet with conductance σ_{\square} . If the conducting sheet is stationary and the loop is moving with a velocity $\mathbf{v} = v_0 \hat{x}$, the electric field in the sheet's frame of reference is given by $\mathbf{E}(\mathbf{r}) =$

$-\mathbf{v} \times \mathbf{B}(\mathbf{r})$ where $\mathbf{B}(\mathbf{r})$ is the magnetic field associated with the current loop. The electric field inside the conducting sheet gives rise to a current density $\mathbf{j}(\mathbf{r}) = \sigma_{\square} \mathbf{E}_{\parallel}(\mathbf{r})$, where \mathbf{E}_{\parallel} is the component of the induced electric field parallel to the conducting sheet. The magnetic field exerts a Lorentz force on the current density so that the force on the sheet in the plane of the sheet is given by

$$F_x(\mathbf{r}) = \int \sigma_{\square} v_0 B_{\perp}^2(\mathbf{r}) ds, \quad (1)$$

where B_{\perp} is the component of the magnetic field perpendicular to the film and the integral is a surface integral over the entire film. This argument neglects the screening response of the conductor to shield the changing magnetic field, but our calculations indicate that for $v_0 \ll c^2 \epsilon_0 / \sigma_{\square}$ the screening current density is small.⁵ The direction of the force on the film is the same as the direction of \mathbf{v} and a reactionary drag force opposes the motion of the loop.

If the motion of the loop is given by $\mathbf{x} = x_0 \sin(\omega t) \hat{x}$, then the velocity is $x_0 \omega \cos(\omega t) \hat{x}$, where ω is the angular frequency and x_0 is the maximum amplitude of oscillation. For this oscillatory motion Eq. (1) becomes

$$F_x(\mathbf{r}, t) = \cos(\omega t) \int \sigma_{\square} \omega x_0 B_{\perp}^2(\mathbf{r}) ds. \quad (2)$$

For uniform metallic films much larger than the loop size, the eddy current dynamometer can be used to determine the conductance of the film since the force is proportional to the conductance.

With the introduction of inhomogeneities in the conducting film, Eq. (2) becomes invalid. For example, if the oscillating current loop is scanned over an edge or crack in the film, the component of the induced current density perpendicular to the edge must be zero ($j_{\perp} = 0$). This boundary

^{a)}Present address: Department of Physics, Indiana University Purdue University Indianapolis, Indianapolis, IN 46202.

condition leads to a directional dependence of the scans depending on whether the direction of oscillation is perpendicular or parallel to the edge or crack. The complete solution of the problem with the boundary conditions included is difficult and beyond the scope of this paper.

The experimental setup and principle of operation of the eddy current dynamometer are described in Sec. II. Section III presents results on several samples with inhomogeneities in the metallic film which demonstrate the spatial resolution, orientational dependence, and sensitivity of the instrument. The fundamental limitations and potential improvements to the instrument are described in Sec. IV.

II. EXPERIMENTAL SETUP

Using Eq. (2), we first estimate the magnitude of the force expected on a copper film. The conductance of 1 μm thick Cu at room temperature is $\sim 58 \Omega^{-1}$. To simplify these estimates, we assume that the magnetic field from the probe is perpendicular to the film and is 0.5 T for $r \leq 50 \mu\text{m}$ and 0 T for $r > 50 \mu\text{m}$. If the probe is spatially vibrating with a frequency of 5000 Hz and an amplitude of 100 nm then Eq. (2) yields a force of 0.34 nN on the film.

High- Q mechanical oscillators made from Si were chosen to measure these small forces.⁶ The mechanical oscillators are made from 0.5 mm thick $\langle 100 \rangle$ Si wafers anisotropically etched in KOH using a lithographically patterned Si_3N_4 layer as a mask. After the KOH has etched through the 0.5 mm wafer, the Si_3N_4 layer is removed. Since the amplitude of vibration is measured capacitively, 15 nm of Cr and 150 nm of Au are evaporated on the oscillators. Details of the fabrication process have been described elsewhere.⁷

A conducting sample, mounted on a glass cover slide, is glued to the end of the Si mechanical oscillator in the configuration shown in Fig. 1(a). The sample and oscillator can be regarded as an effective harmonic oscillator⁸ which is driven at the resonant frequency of the fundamental cantilever mode using the eddy current force induced by an oscillating magnetic probe.

The magnetic probe (tip) is an iron wire (o.d.=0.9 mm) mechanically polished with 1 μm grit down to a tip diameter of 20 μm that localizes the magnetic flux from a neodymium iron boron permanent magnet (1/4 in. diameter by 1/4 in. long). To repair damage from the polishing process, the wire is annealed in a hydrogen furnace at 1000 $^\circ\text{C}$ as described in Ref. 9. The hydrogen anneal decreases the full width half maximum (FWHM) of the magnetic field profile and increases the maximum magnetic field. This profile, shown in Fig. 2, was measured by scanning a 10 μm Hall bar under the tip, at a tip-Hall bar separation of 10 μm . The FWHM of the magnetic field profile is approximately 80 μm .

The permanent magnet and iron tip are fastened to the top of a piezoelectric quadrant tube as shown in Fig. 1(a). The tube is used to vibrate the iron tip at the resonant frequency of the oscillator by applying an alternating current (ac) voltage from a signal generator. The magnetic tip was manufactured to have a resonant frequency near the Si mechanical oscillator's resonant frequency to increase the vibra-

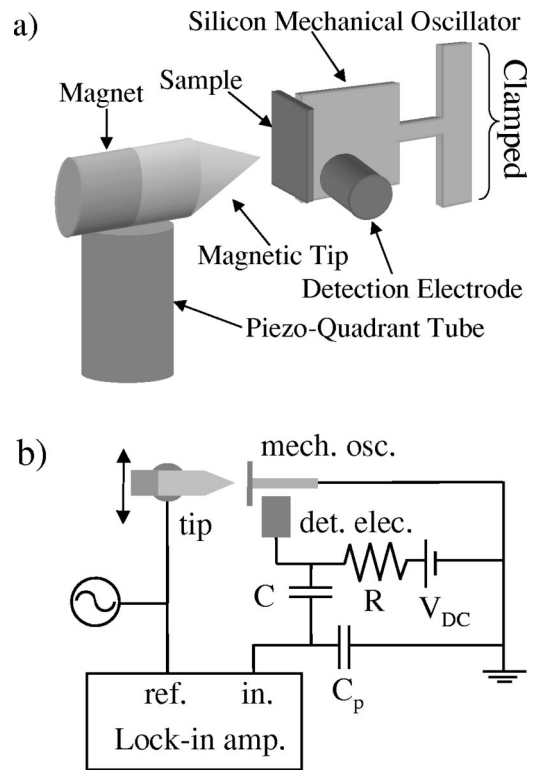


FIG. 1. Sketch of the experimental setup. (a) A conducting sample is glued to a Cr and Au coated Si mechanical oscillator. A permanent magnet and a ferromagnetic needle, used to localize the magnetic flux, are attached to the top of a piezoelectric quadrant tube which is vibrated at the oscillator's resonant frequency. The amplitude of vibration of the mechanical oscillator is measured capacitively with a detection electrode. (b) Block diagram of the electronics used in the experimental setup. $R=5 \text{ M}\Omega$, $C=0.22 \mu\text{F}$, $V_{dc} \sim 90 \text{ V}$, and $C_p \sim 130 \text{ pF}$.

tional amplitude of the tip and consequently the force on the metallic film [see Eq. (2)].

The oscillating eddy current force from the vibrating magnetic tip causes the sample and Si mechanical oscillator to vibrate. The motion of the Si oscillator is measured capacitively using a detection electrode and the circuit shown in Fig. 1(b). If the oscillator moves a distance δd then the

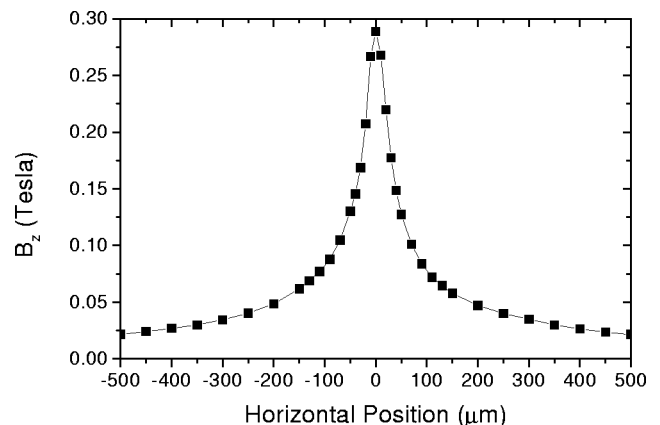


FIG. 2. The z component of the magnetic field profile of a sharpened iron tip. The profile was measured with a 10 μm Hall bar for a 10 micron tip-Hall bar separation. The FWHM is 80 μm . The physical diameter of the tip is 20 μm . The source of the magnetic field is a neodymium iron boron permanent magnet.

electrode oscillator capacitance changes by $\delta C \cong -C_0 \delta d/d$, where C_0 (~ 1 pF) is the electrode-oscillator static capacitance and d is the distance between the oscillator and electrode at equilibrium, $d \gg \delta d$. When the electrode is biased to a dc voltage ($V_{dc} \sim 90$ V), the change in voltage between the electrode and the oscillator is directly proportional to the motion of the oscillator. The amplitude of the ac voltage is given by¹⁰

$$\delta V \cong -\frac{\delta C}{C_T} V_{dc} \cong \frac{C_0}{C_T} \frac{\delta d}{d} V_{dc}, \quad (3)$$

where C_T is the sum of C_0 and a parallel external parasitic capacitance ($C_p \sim 100$ pF) which is dominated by cable and preamplifier capacitance to ground. For these measurements, $\delta d/\delta V$ was calibrated directly by measuring the amplitude of the oscillator with an optical interferometer. The values, while constant during each scan, ranged from 70–400 pm/ μ V for different scans due to a variance in the oscillator-electrode spacing.

The signal from Eq. (3) is measured using a lock-in amplifier with the signal generator as reference. Once the amplitude of the oscillator is recorded, the tip is moved to a new location over the sample. In this way, the spatial dependence of the eddy current force on the sample is determined.¹¹ In the next section, we show how the resonant amplitude of the Si mechanical oscillator changes as the iron tip is scanned across different samples.

III. RESULTS

To demonstrate the capabilities of the instrument, we present results of measurements on copper films with different inhomogeneities. The inhomogeneities are single and double slits in 12.5 and 25 μ m thick Cu.¹² Figure 3(a) shows two scans of a 1 mm wide 25 μ m thick copper ribbon. In the middle of the ribbon the amplitude of the Si oscillator is (0.556 ± 0.007) nm. The noise has been defined as the root mean square (rms) difference between neighboring points in the amplitude of the oscillator when the tip is near the center of the ribbon. The reproducibility when comparing two scans over the same strip is also approximately 10 pm.

At resonance, the force acting on the sample, and therefore on the Si oscillator, is $F = (k/Q)A$, where k is the spring constant, Q is the quality factor, and A is the measured amplitude of the oscillator. The spring constant was measured to be $k = (12\,000 \pm 300)$ N/m by noting the change in resonant frequency when known masses were added to the oscillator. The quality factor was 460 for the scan¹³ in Fig. 3(a) yielding $F_{\text{eddy}} = 15$ nN.

The theoretical eddy current force can be estimated using Eq. (2), the measured magnetic field profile from Fig. 2, and the measured amplitude of the tip. Using Eq. (2) for this estimation neglects the screening currents and boundary effects on the current density by assuming the sample to be infinite. Using the magnetic field profile from Fig. 2, $\int \int B^2(x,y) dx dy \approx 1.2 \times 10^{-9}$ T²m². The velocity of the tip¹⁴ is 6.9×10^{-3} m/s and therefore the expected force is 12 nN, which is in good agreement with the experimental value.

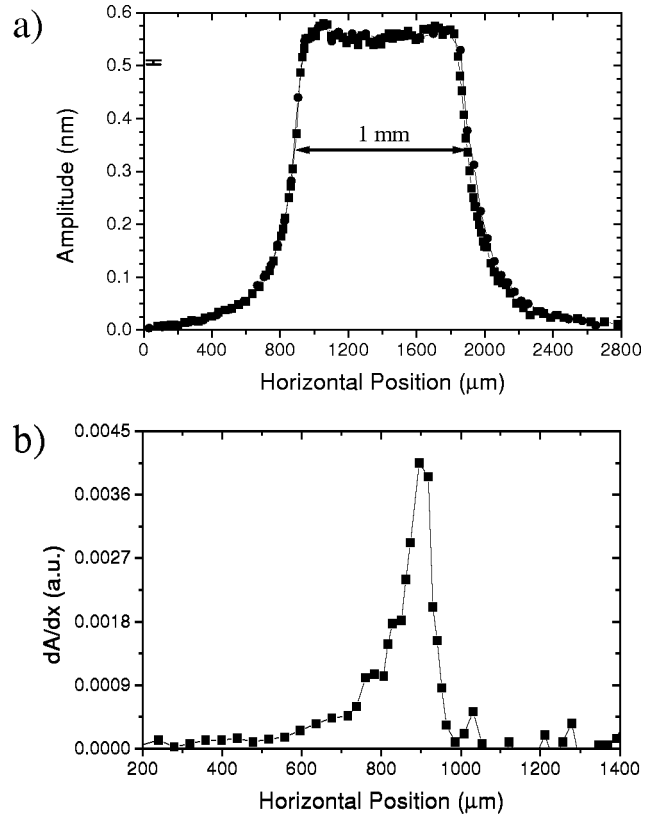


FIG. 3. (a) Two scans over a 1 mm wide 25.4 μ m thick Cu ribbon. The amplitude of motion of the mechanical oscillator when the tip is in the middle of the ribbon is (0.556 ± 0.007) nm. The reproducibility in the amplitude when comparing the two data sets is approximately 0.01 nm. (b) Spatial derivative of the left edge for the scan in (a). FWHM is ≈ 80 μ m.

Assuming that the boundaries are not affecting the magnitude of the signal when the tip is over the center of the Cu ribbon, we can estimate the equivalent noise conductance of the instrument. Taking the observed noise to be $0.01/0.556 \approx 0.02$ and the known conductance of the Cu ribbon, the equivalent noise conductance is $\Delta \sigma_{\square} \cong 30 \Omega^{-1}$.

The eddy current force is observed to persist for a long distance as the tip is scanned over the edge (≈ 900 μ m to go to zero for this tip). This slow decay of the eddy current signal is thought to be due to the long tail in the magnetic field profile of the magnetic tip. Experiments show that this long tail is not due to the permanent magnet, and computer simulations of this profile indicate that this tail is not intrinsic to the tip shape and can be further decreased. This might be carried out by annealing the tips longer or by fabricating the tips differently (e.g., chemically etching the tips). This large tail, however, does not limit the resolution of the instrument, as discussed in the next section.

A. Resolution and crack detection

The expected spatial resolution of the instrument is determined by taking the spatial derivative of the data from the scan over an edge. By measuring the FWHM of that derivative the expected spatial resolution can be deduced. Figure 3(b) shows the numerical derivative of an edge for the scan over the 1 mm Cu ribbon [Fig. 3(a)]. The FWHM of that

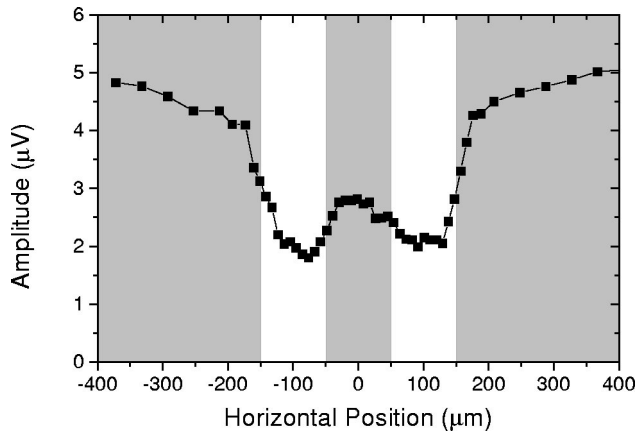


FIG. 4. Scan over two $100\ \mu\text{m}$ wide slits separated by $200\ \mu\text{m}$ in $12.7\ \mu\text{m}$ thick Cu. The amplitude of the tip was $550\ \text{nm}$ and the Q of the oscillator was 860 .

derivative is approximately $80\ \mu\text{m}$, which is in good agreement with the FWHM of the magnetic field profile.

To demonstrate this spatial resolution, a Cu sheet with a double slit was scanned. The sample has two $100\ \mu\text{m}$ wide slits separated by $200\ \mu\text{m}$ in $12.7\ \mu\text{m}$ thick copper foil. The results from this scan are shown in Fig. 4. This scan demonstrates that the spatial resolution of the instrument is $\approx 100\ \mu\text{m}$ since it reveals two minima separated by a local maximum.

The discussion so far has been on scans performed with the oscillation of the tip perpendicular to the edge. An important extra feature of the instrument arises when the oscillatory tip motion is parallel to the sample edge. The perpendicular (parallel) orientation is defined as when the oscillation of the tip is perpendicular (parallel) to an edge (see Fig. 5).

An experiment to determine whether the instrument was sensitive enough to measure a break or a crack in the film was done. For this measurement, a $2.5\ \mu\text{m}$ wide slit in $12.7\ \mu\text{m}$ thick copper was used. Since the slit is much smaller

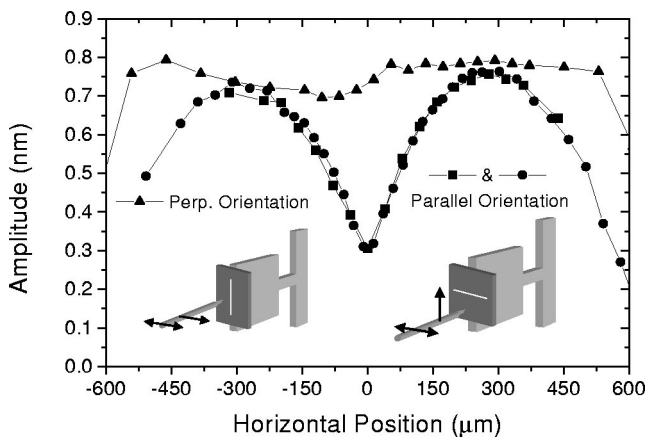


FIG. 5. Scans over a $2.5\ \mu\text{m}$ wide slit in $12.7\ \mu\text{m}$ thick Cu for the two different orientations. The perpendicular (parallel) orientation corresponds to the oscillation of the tip perpendicular (parallel) to an edge or crack in the metallic film. The inset pictorially demonstrates the difference between the two. The single arrow labels the scan direction while the double arrow labels the direction of oscillation. The amplitude of the tip was $620\ \text{nm}$ and the Q of the oscillator was 700 .

than the resolution, a scan over this slit is equivalent to a scan over an infinitesimal crack. Figure 5 is a scan over the $2.5\ \mu\text{m}$ slit for the two different orientations.

In the perpendicular orientation, the instrument is not able to detect the slit within the noise of the instrument. For the parallel orientation, however, the slit is clearly observed. The signal decreases on the left- and right-hand side in this figure because of the outer edges in the Cu film. This figure demonstrates that the parallel orientation is very sensitive to edges or breaks in the film, even for a slit much smaller than the resolution of the instrument.

The differences between the two orientations can be understood qualitatively. The component of the current density perpendicular to an edge must be zero. In the perpendicular orientation the induced electric field is parallel to the edges of the slit and therefore the boundary condition does not drastically reduce the current density inside the film. For the parallel orientation the induced electric field is perpendicular to the edges. In this configuration the current density in the film is severely modified to adjust to the boundary conditions.

To test the sensitivity of the instrument to weaker inhomogeneities, a trench $23\ \mu\text{m}$ deep by $25\ \mu\text{m}$ wide in a $40\ \mu\text{m}$ thick Cu layer was scanned in the parallel orientation. In this case no evidence for the trench could be detected in the SECD signal. We conclude that because of the current flow underneath the trench the overall current pattern is not appreciably perturbed.

IV. DISCUSSION

In this section the fundamental limitations and improvements to the instrument are discussed. Thermal noise sets the ultimate limit on the minimal amplitude that can be measured with the mechanical oscillator and the equipartition theorem gives

$$\langle x^2 \rangle^{1/2} = \sqrt{\frac{k_B T}{k}} \cong 0.6\ \text{pm rms}, \quad (4)$$

where $T = 300\ \text{K}$ is the temperature of the system, k_B is the Boltzmann constant, and $\langle x^2 \rangle^{1/2}$ is the thermal root mean square of the amplitude of the oscillator. Equation (4) assumes that the bandwidth of the measurement is self-limited by the oscillator, $B = \pi f_0 / 2Q$, where f_0 is the resonant frequency of the oscillator. If the bandwidth of the lock-in amplifier, Δf , is much smaller than the oscillator's bandwidth, the thermal noise equivalent amplitude is

$$\frac{\langle x^2 \rangle^{1/2}}{\sqrt{\Delta f}} = \sqrt{\frac{2Qk_B T}{\pi f_0 k}} \cong 0.2\ \text{pm rms}/\sqrt{\text{Hz}}. \quad (5)$$

In practice, noise from the preamplifier used to measure the induced voltage of the oscillator limits the minimal amplitude that can be measured while the tip is stationary. The preamplifier noise was $\approx 10\ \text{nV rms}/\sqrt{\text{Hz}}$, which corresponds to a noise equivalent amplitude between $(0.7\ \text{and}\ 4)\ \text{pm rms}/\sqrt{\text{Hz}}$, where the range is due to a variance in the electrode-oscillator capacitance. Another source of noise in these mea-

surements was reproducibility of the tip-sample separation when scanning the tip over the sample. This is the source of noise that dominated the scans in Fig. 3.

The force sensitivity of the oscillator can be enhanced by an increase in the Q of the oscillator. Since the force at resonance is equal to $F=(k/Q)A$, an increase in Q corresponds to an increase in the amplitude of the oscillator for the same force applied to the oscillator. Quality factors as large as 3×10^6 have been reported for similar Si mechanical oscillators,⁴ corresponding to a factor ~ 5000 increase in the sensitivity of our force measurements.

An improvement in the sensitivity would allow the spatial resolution of the instrument to be increased. A spatial resolution on the order of $1 \mu\text{m}$ would make the eddy current dynamometer a versatile instrument, although a tip with a FWHM equal to $1 \mu\text{m}$ in the magnetic field profile would have to be developed to get this resolution. With $Q \sim 10^6$ and a spatial resolution on the order of $1 \mu\text{m}$, the expected noise equivalent conductance is $\Delta\sigma_{\square} \approx 30 \Omega^{-1}/\sqrt{\text{Hz}}$ when imaging a sample large compared to the tip size. With this sensitivity, we should be able to measure the conductance of sub-micron thick metals at 4 K.

Finally, a further theoretical understanding of the eddy current force in the presence of conductive inhomogeneities for a moving magnetic probe could allow the deconvolution of these scans to determine the conductance of the sample as a function of position.

ACKNOWLEDGMENTS

The authors would like to acknowledge both C. H. Yang from the University of Maryland and L. Krusin-Elbaum from IBM T. J. Watson Research Center for providing Hall bars to make the magnetic field measurements. The authors are in-

debted to R. Frizzell for providing assistance in making the tips and are grateful to O. King and S. Horst for providing technical advice and assistance in the manufacture of the oscillators.

¹H. L. Libby, *Introduction to Electromagnetic Nondestructive Test Methods* (Wiley-Interscience, New York, 1971).

²R. C. Black, F. C. Wellstood, E. Dantsker, A. H. Miklich, J. J. Kingston, D. T. Nemeth, and J. Clarke, *Appl. Phys. Lett.* **64**, 100 (1994).

³A. N. Cleland and M. L. Roukes, *Nature (London)* **392**, 160 (1998).

⁴R. D. Biggar and J. M. Parpia, *Rev. Sci. Instrum.* **69**, 3558 (1998).

⁵B. S. Palmer, R. S. Decca, and H. D. Drew (unpublished results). Calculations are based on J. R. Reitz, *J. Appl. Phys.* **41**, 2067 (1970); W. M. Saslow, *Am. J. Phys.* **60**, 693 (1992).

⁶R. N. Kleiman, G. K. Kaminsky, J. D. Reppy, R. Pindak, and D. J. Bishop, *Rev. Sci. Instrum.* **56**, 2088 (1985).

⁷G. Kaminsky, *J. Vac. Sci. Technol. B* **3**, 1015 (1985); K. E. Bean, *IEEE Trans. Electron Devices* **ED-25**, 1185 (1978).

⁸K. Karrai and R. D. Grober, *Appl. Phys. Lett.* **66**, 1842 (1995); R. S. Decca, H. D. Drew, and K. L. Empson, *Rev. Sci. Instrum.* **68**, 1291 (1997).

⁹R. M. Bozorth, *Ferromagnetism* (IEEE, New York, 1993).

¹⁰G. K.-S. Wong, in *Experimental Techniques in Condensed Matter Physics at Low Temperatures*, edited by R. C. Richardson and E. N. Smith (Addison-Wesley, Redwood City, CA, 1988), Chap. 4.2.

¹¹Another potential experimental setup would be to mount the magnetic tip on the Si mechanical oscillator, vibrate the Si oscillator and magnetic tip, and measure the change in amplitude while the tip is scanned over the sample. The problem with this setup is that the change in the amplitude due to magnetic drag is small compared with the original amplitude and is estimated to be on the order of one part per thousand for the measurements presented here.

¹²National Aperture, Inc., 26 Keewaydin Dr., Ste. B, Salem, NH 03079.

¹³The quality factor, while constant during each scan, was found to vary from approximately 400 to 1000. The variance in the quality factor is associated with cleanliness during the mounting of samples to the oscillator.

¹⁴The amplitude of the tip can be considered to be a constant during the scans since the change due to magnetic drag is much smaller (less than 100 ppm) than the original amplitude.